Quaternary International xxx (2017) 1–15

Contents lists available at ScienceDirect

Quaternary International

journal homepage: www.elsevier.com/locate/quaint

A complex thrust sequence in western Himalaya: The active Medlicott Wadia Thrust

J.-L. Mugnier [c, d, *], V. Vignon [a], R. Jayangondaperumal [f], R. Vassallo [c, d], M.A. Malik [e], A. Replumaz [a, b], R.P. Srivastava [f], F. Jouanne [c, d], J.F. Buoncristiani [g], H. Jomard [h], J. Carcaillet [a, b]

[a] Univ. Grenoble Alpes, ISTerre, F-38041 Grenoble, France
[b] CNRS, ISTerre, F-38041 Grenoble, France
[c] Université de Savoie-Mont-Blanc, ISTerre, F-73376 Le Bourget du Lac, France
[d] CNRS, ISTerre, F-73376 Le Bourget du Lac, France
[e] Department of Geology, University of Jammu, India
[f] Wadia Institute of Himalayan Geology, Dehra Dun, India
[g] CNRS, Biogeosciences, University of Burgundy, France
[h] Institut de Radioprotection et de Sûreté Nucléaire (IRSN), France

ARTICLE INFO

Article history:
Received 14 March 2016
Received in revised form
6 April 2017
Accepted 17 May 2017
Available online xxx

Keywords:
Thrust splay
Earthquake
Active fault
Himalaya
Out-of-sequence thrust
In-sequence thrust

ABSTRACT

The recent activity of the Medlicott-Wadia Thrust (MWT) is investigated by geomorphic and tectonic studies in the Riasi zone, south of the Pir Panjal range (India, Jammu-Kasmir state of western Himalaya). In the Riasi area, the MWT forms a splay of five faults that dip northward. The recent activity of the splay is quantified using a set of deformed Quaternary alluvial units. The central branch of the thrust splay moved Precambrian limestones above Quaternary sediments and is sealed by 36 ± 3 ka (youngest OSL age) deposits. The other branches offset the top of a 15 ± 1 ka (youngest OSL age) alluvial fan by 180 to 120 m; the two southernmost branches form 17–34 m high non-cylindrical scarps and the two northernmost branches also offset the fan by ~8 m and ~54 m, respectively. A balanced cross-section parallel to the N210°E thrust motion suggests that the sequence of activity is complex: an in-sequence propagation is found for the three southern Tea, Scorpion and Rain faults and an out-of-sequence reactivation for the northern Pillar fault. Furthermore, several thrusts simultaneously activated for intervals of a few thousand years, whereas others are episodically inactive. Nearly 10 mm/yr of India-Eurasia convergence is regularly absorbed by the MWT, a value greater than the one estimated for the western segment of the MWT affected by the 2005 Kashmir earthquake, where the thrust tectonics interacts with the complex kinematics of the syntax. This work indicates that the MWT is very active and might be related to thick-skinned tectonics in the western Himalaya.

1. Introduction

The present-day tectonism of the Himalaya is characterized by the under-thrusting of the Indian lithosphere below the Main Himalayan Thrust (MHT; e.g. Coward et al., 1986; Zhao and Nelson, 1993). Historical archives indicate that large earthquakes with a magnitude of Mw ~8 have episodically ruptured several hundred km-long segments of the MHT (Chandra, 1992). These large events have been used to define a Himalayan seismic model in which the elastic stress accumulated in the upper crust during interseismic periods is released and propagates toward the frontal structure, the Main Frontal Thrust (MFT) (Avouac, 2003; Feldl and Bilham, 2006). Nonetheless, large earthquakes have also occurred north of this front, like the 2005 Mw 7.6 earthquake in Kashmir that ruptured a thrust ~100 km north of the MFT (Kaneda et al., 2008); these earthquakes occur along "out-of-sequence" thrusts (Mugnier et al., 2005; Mukherjee, 2015) The pattern of historical earthquakes leaves significant seismic gaps (Seeber and Armbruster, 1981) and the major gap in the western Himalaya is located between the rupture areas of the 1905 Kangra earthquake (Hough and Bilham,

* Corresponding author. Université de Savoie-Mont-Blanc, ISTerre, F-73376 Le Bourget du Lac, France.
E-mail address: jean-louis.mugnier@univ-savoie.fr (J.-L. Mugnier).

http://dx.doi.org/10.1016/j.quaint.2017.05.028
1040-6182/

2008) and the 2005 Kashmir earthquake that affected zones on both sides of the line of fire between India and Pakistan (Hussain et al., 2009). The Jammu-Kashmir area has not experienced any major events since the Mw > 7 Srinagar earthquake in 1555 (Ambraseys and Douglas, 2004) and thus is a potential spot for a great earthquake rupture. Within this seismic gap area, the Medlicott-Wadia Thrust (MWT) (Thakur et al., 2010) lies between the Main Frontal Thrust (MFT) and the Main Boundary Thrust (MBT) (Fig. 1). This latter thrust was affected by the 2005 Kashmir earthquake (Kaneda et al., 2008) and paleo-events (Kondo et al., 2008; Vassallo et al., 2013) and has been active since at least 36 ka (Vignon et al., 2016).

Few active faults have been recognized in the western Himalaya (Yeats et al., 1992; Vassallo et al., 2015) and the aim of this paper is to quantify the tectonic activity of the MWT in the seismic gap of the western Himalaya and more specifically close to its intersection with the Chenab River (Fig. 1). The thrust is there referred to as the Riasi Thrust (Thakur et al., 2010). We investigate whether the out-of-sequence 2005 earthquake (Kondo et al., 2008) was a singularity in the western syntax (Pêcher et al., 2008), or whether it can be considered as being typical of out-of-sequence seismic ruptures (Mugnier et al., 2005) in the western Himalaya. In this latter case, not all of the great earthquakes would rupture the MHT from the ductile/brittle transition to the most frontal structure (i.e. the MFT), as inferred by the seismo-tectonic model (Avouac, 2003) but some ruptures would take place along out-of-sequence thrusts. Finally, a model that takes out-of-sequence ruptures into account is discussed in order to understand the origin of the Jammu-Kashmir seismic gap and to infer its seismic hazard implications.

2. Geological and geomorphologic results

2.1. Geology of the area

The Pir Panjal range rises to 5572 m and is located between the

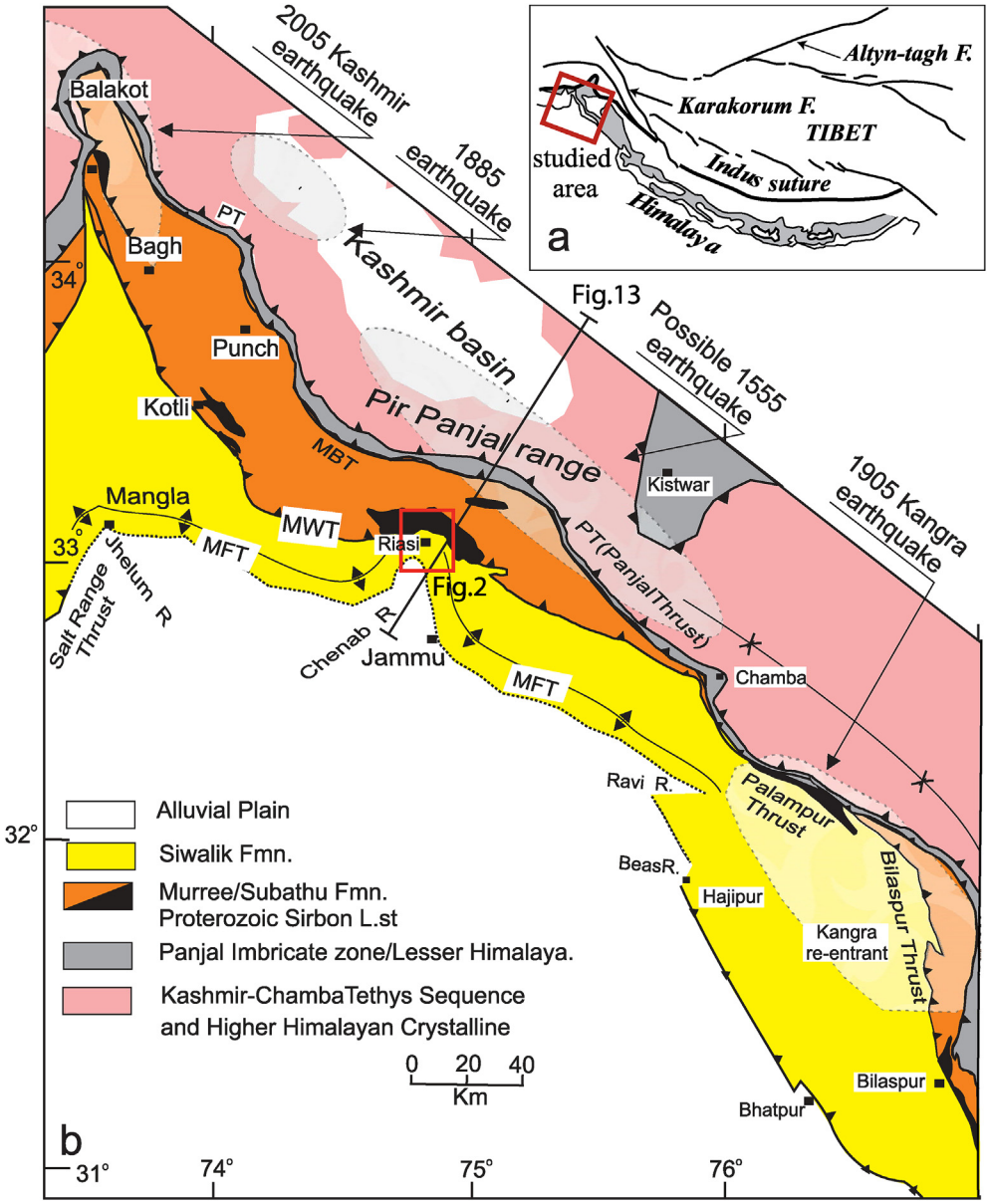

Fig. 1. (a) Location of the studied area in the Himalaya; b) Geological map of the northwest Himalaya (modified after Thakur et al., 2010) showing the 1905 Kangra and 2005 Kashmir earthquake ruptures (from Hough and Bilham, 2008; Bendick et al., 2007; respectively) and the inferred 1885 and 1555 paleoseisms events in the Kashmir area (from Joshi and Thakur, 2016). PT: Panjal Thrust and Main Central Thrust; MBT: Main Boundary Thrust; MWT: Medlicott-Wadia Thrust; MFT: Main Frontal Thrust.

Please cite this article in press as: Mugnier, J.-L., et al., A complex thrust sequence in western Himalaya: The active Medlicott Wadia Thrust, Quaternary International (2017), http://dx.doi.org/10.1016/j.quaint.2017.05.028

Kashmir Basin and the Indian plain (Fig. 1b). Several northward-dipping thrusts are located on the southern flank of this range and branch off the MHT; the MWT is one of them. There are very few data about the geometry of the MHT in the western Himalaya. Nonetheless, studies of the 2005 Kashmir earthquake indicate that the MWT is a ramp branching off the MHT at a depth of ~15 km (Avouac et al., 2006) and a flat affected by post-seismic creep (Jouanne et al., 2011) extends north-west of the Kashmir basin. The hangingwall of the MWT is mainly formed by the Paleocene to Miocene Murree Formation. In the Chenab area, Precambrian limestones (Gansser, 1964; Krishnaswamy et al., 1970) form the hangingwall of the Riasi thrust (Fig. 1b) and the limestone bedding generally dips steeply northeastward.

The foothills between the alluvial plain of the foreland and the MWT are formed of folded Siwalik deposits (Mugnier and Huyghe, 2006). The main structure is a ~20 km wide anticline and its present-day growth is proved by uplifted terraces (Vassallo et al., 2015). No thrust reaches the surface south of the frontal anticline. Nonetheless, this anticline is not related to a simple fault-propagation fold (Mugnier et al., 1992; Champel et al., 2002) but rather to a complex splay of faults imaged in the core of the anticline by seismic profiles (e.g. Raiverman et al., 1994; Srinivasan and Khar, 1996); these blind structures are presumably the local expression of the MFT.

The structures trend N130°E at the regional scale but the frontal anticline and the MWT are affected by a recess (Marshak, 2004) close to Jammu (Fig. 1b). The amplitude of the recess in map-view partly results from the incision by the Chenab River that flows at its apex; this amplitude is furthermore lower for the MWT than for the frontal structure and the distance between the MHT and the plain is only ~15 km along the Chenab River, versus ~40 km in the zones where the structures trend N130°E (Fig. 1b). The MWT cuts through minor folds of the Siwaliks, confirming that it postdates these folds and is out-of-sequence with respect to the frontal structure. Furthermore, an unconformity above the frontal anticline has been dated at 1.7 Ma by magnetostratigraphy (Johnson et al., 1979) and indicates that this structure was active during the entire Quaternary. Close to the town of Riasi, the footwall of the MWT is composed mainly of fluvial sediments deposited above the Siwaliks and the deformation is distributed along several branches of a thrust splay (Fig. 2b).

2.2. Mapping of the active faults

SPOT satellite images, together with field mapping, were used to map the faults and sedimentary units in the Riasi area.

The mapping, description and dating of 15 sedimentary and terraces units is presented in detail by Vignon et al. (2016). Their description (Fig. 3) takes into account: (1) their position in relation to the Riasi thrust (i.e. F: Footwall; H: Hangingwall); (2) their relative altitude above the present-day riverbed (0 for the higher terrace, 5 for the lower terrace); (3) the river at the origin of the deposition (i.e. the Chenab, Anji or Nodda Rivers). Furthermore 12 sites were dated (Table 1). Most of them are presented and discussed by Vignon et al. (2016). These 12 sites can be used to determine the absolute ages of three major units at ~36–38, 14–15 and 4 ka, respectively (Figs. 2b and 3). The largest terrace level, where the city of Riasi is built, was deposited around 15 ka by the Anji River, a large tributary of the Chenab River (Fig. 2b).

The terrace units directly affected by the faults and the relationships between the faults and terraces are described in detail below (Fig. 4).

2.2.1. Chenab units

Two sedimentary units are located beneath the Nodda fan. They

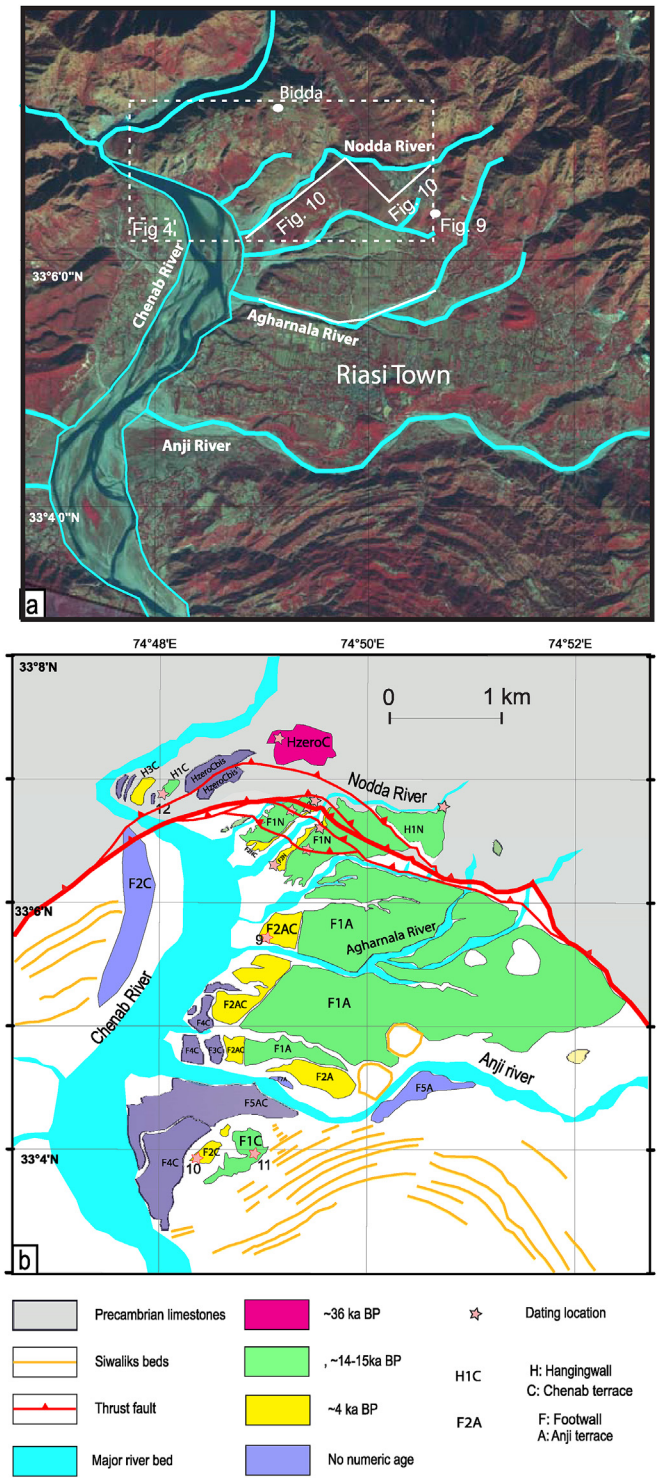

Fig. 2. Morphotectonic map of the Riasi area. (a) Satellite image (SPOT) of the study area with location of the other figures. (b) Morphotectonic and geochronologic interpretation of the Riasi area (adapted from Vignon et al., 2016). The color of the terraces refer to their age: purple, green and yellow for ~36 ka BP, ~14-15ka BP and ~4 ka BP, respectively. The detailed nomenclature of the sedimentary units (see Fig. 3) refers to the position in relation to the Riasi thrust, the relative altitude above the present-day riverbed and the river at the origin of the deposition. (For interpretation of the references to colour in this figure legend, the reader is referred to the web version of this article.)

Please cite this article in press as: Mugnier, J.-L., et al., A complex thrust sequence in western Himalaya: The active Medlicott Wadia Thrust, Quaternary International (2017), http://dx.doi.org/10.1016/j.quaint.2017.05.028

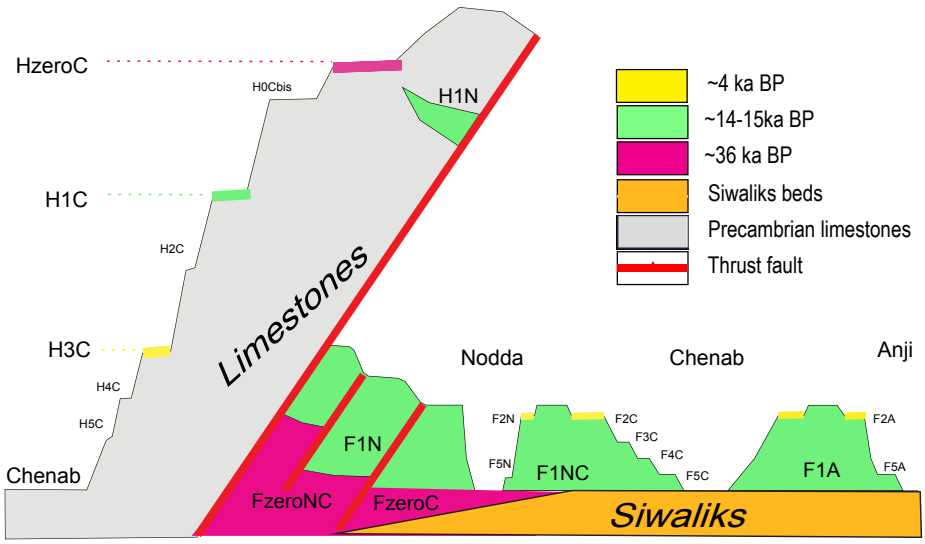

Fig. 3. A sketch of the relationships between the terrace units and faults in the Riasi area (adapted from Vignon et al., 2016). Detailed sedimentary unit names depend on: (1) the position in relation to the Riasi thrust (i.e. F: Footwall; H: Hangingwall); (2) the relative altitude above the present-day riverbed. (i.e. zero for highest, 2 for lowest). Note that two different numbering systems were used for the footwall and hangingwall of the thrust. (3) The river at the origin of the deposition (i.e. C: Chenab; A: Anji; N: Nodda). The color of the terraces refer to the simplified interpretation of the numeric ages (unit ~36ka, unit 14-15ka and unit 2 4ka). (For interpretation of the references to colour in this figure legend, the reader is referred to the web version of this article.)

Table 1
List of the sites where dating has been performed (location in Figs. 2b and 4b).

Dated Site	Terrace Name	Location	Method	Reference	Sample name	Age (ka)
Units ~ 36 ka						
1	HzeroC	North side terrace	OSL (youngest)	Vignon et al., 2016	K2-12	36 ± 5
1	HzeroC	North side terrace profile	10Be	Vignon et al., 2016	JK.08.15, JK.08.11, JK.08.08, JK.08.07, JK.08.05, JK.08.04, JK.08.03	>21
2	FzeroC	Nodda gorge	OSL (youngest)	Vignon et al., 2016	JK-10-32	36 ± 3
3	FzeroNC	Nodda gorge	OSL (youngest)	Vignon et al., 2016	JK-10-31	38 ± 3
Units ~14–15 ka						
4	H1N	Trench in the surface terrace	OSL (youngest)	Vignon et al., 2016	JK-10-80	15 ± 1
5	F1N	Nodda gorge	OSL (youngest)	Vignon et al., 2016	JK-10-33	14+/2
6	F1N	Trench in the surface terrace	OSL (youngest)	Vignon et al., 2014	Dag2, Dag5, Dag9	12–18.6
7	F1N	Trench in the surface terrace	14C	Vassallo et al., 2013	LMC14-K12-17	13.9 ± 0.07
11	F1C	North side terrace profile	10Be	Vignon, 2011	JK 10 36, JK 10 37, JK 10 38, JK 10 42, JK 10 55, JK 10 56	13–21
12	H1C	Surface terrace	10Be	Vignon et al., 2016	JK.10.18, JK.10.19	7–16
Units ~4 ka						
8	F2NC	Surface terrace	10Be	Vignon et al., 2016	JK.10.89	2–5.2
9	F2AC	South side terrace profile	10Be	Vignon et al., 2016	JK.08.46, JK.08.47, JK.08.48, JK.08.50, JK.08.44, JK.08.43, JK.08.42, JK.08.37	3.8 ± 0.4
10	F2C	Surface terrace	10Be	Vignon, 2011	JK 10 51, JK 10 52	3.2–6.9

are distinct from the Nodda fan and are mainly formed of Chenab sediments.

Along the Nodda River gorge, the upper unit (FzeroNC in Fig. 5) is deposited upon the limestone and its lower boundary is formed by a rather planar strath surface. This surface dips a few degrees W–NW and therefore lies at a higher level on the eastern side of the Nodda River than on the western side. This upper unit nearly seals the Tea fault located between the Chenab sediments and limestones; furthermore, it lies above other Chenab deposits (FzeroC on Fig. 5) located in the footwall of the fault. The upper boundary of these Chenab-related units is also observed in the core of the anticline in the hangingwall of the Rain fault. OSL dating indicates ages of 36 ± 3 ka and 38 ± 3 ka for these two units, respectively. A time discontinuity of ~20 ka therefore occurred between these units and the ~14–15 ka old Nodda fan.

In the hangingwall of the Riasi thrust, several strath terraces were carved the limestone at the top and on the western side of a spur above a meander of the Chenab River.

The highest terrace (HzeroC in Fig. 4b) is 375 m above the Chenab River and is dated at 36 ± 3 ka. This highest unit is therefore the equivalent in the hangingwall of the Chenab unit found in the footwall (Fzero NC unit in Fig. 5) located close to the Rain fault in the Nodda gorges. HzeroCbis and HzeroC are kilometer-wide flat surfaces (Fig. 2). Another Chenab terrace (HzeroCbis in Fig. 2) is located 330 m above the Chenab River and its southern part (HzeroCbis' in Fig. 2) is offset 15 m downward by the Pillar fault.

2.2.2. Nodda River alluvial fan

The Nodda River catchment is only ~5 km^2 and the river has built an alluvial fan in the vicinity of the Chenab River. A recent

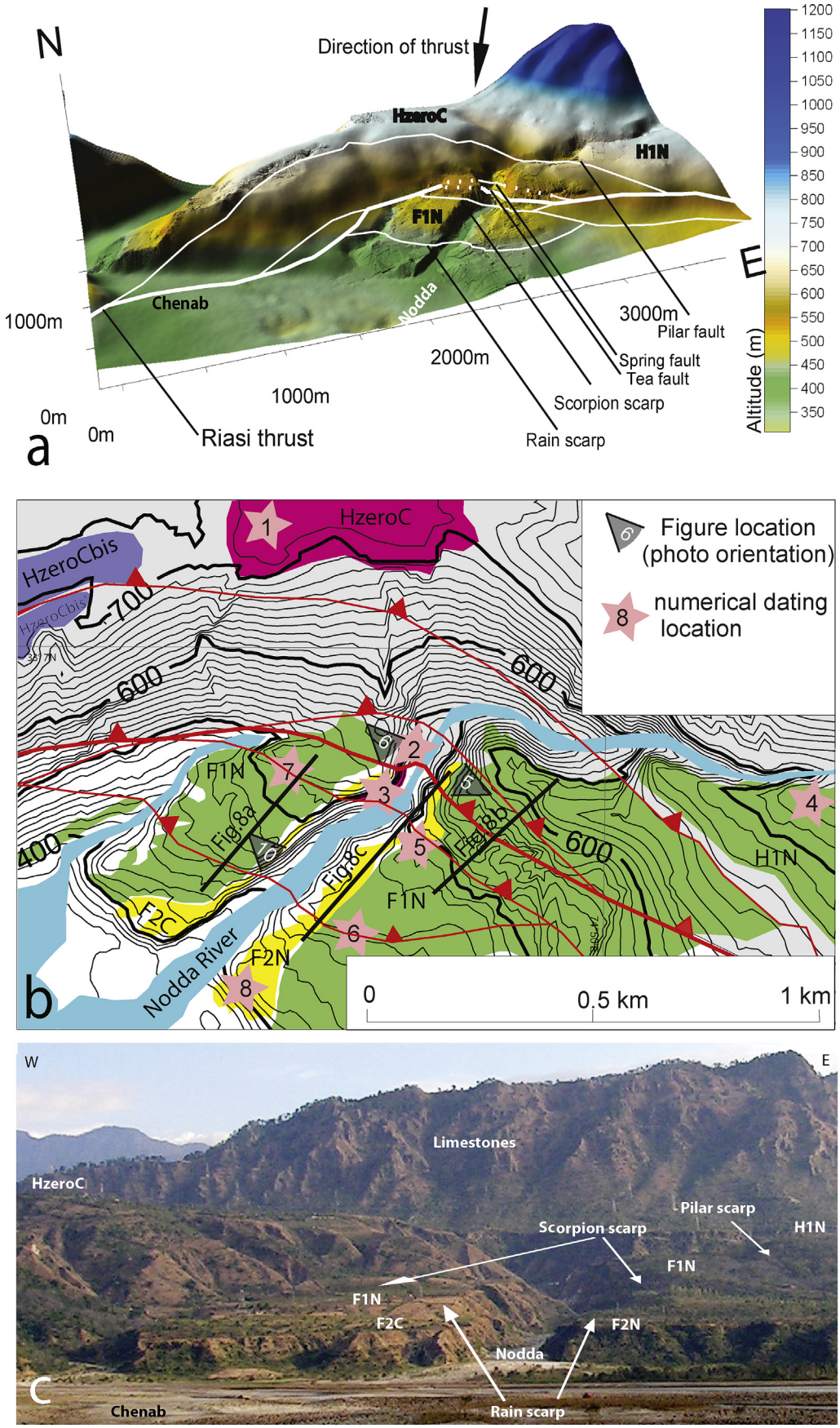

Fig. 4. (a) DEM of the Nodda Fan area built from kinematic GPS data and ASTER GDEM data (blurred part). White lines for the faults, dotted line when sealed by Quaternary deposits, and thick line for the Riasi thrust. (b) Detailed morphotectonic map of the area around the Nodda fan; same caption as Fig. 2b. (c) Picture of the Nodda Fan from the south. The white arrows point to the tectonic scarps of the Rain fault and Scorpion fault.

Please cite this article in press as: Mugnier, J.-L., et al., A complex thrust sequence in western Himalaya: The active Medlicott Wadia Thrust, Quaternary International (2017), http://dx.doi.org/10.1016/j.quaint.2017.05.028

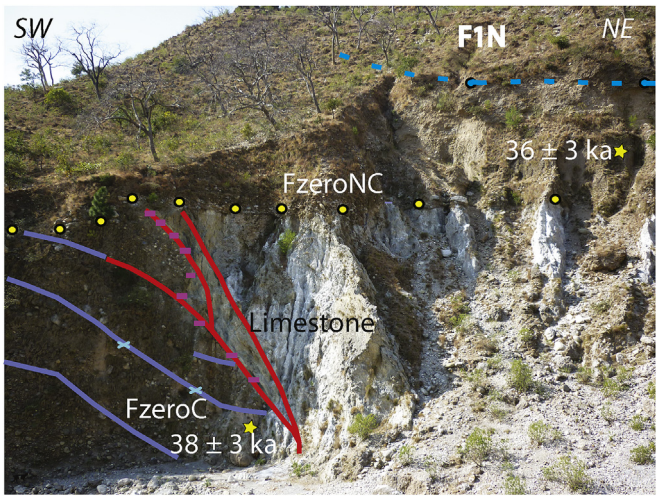

Fig. 5. The Tea fault and the lowest sedimentary units (FzeroC and FzeroNC) observed along the Nodda River; location on Fig. 4b. Continuous blue lines for the Chenab layers, red lines for the fault planes, dashed yellow line for the strath surface above the FzeroC unit and the hangingwall of the Tea fault, dashed blue line for the contact at the base of the F1N unit; light blue crosses, yellow dots and purple dashes for the total station measurement used to construct the cross-sections in Figs. 11 and 12b; yellow stars for the OSL samples (38 ± 3 ka and 36 ± 3 ka for the FzeroC and FzeroNC units, respectively). (For interpretation of the references to colour in this figure legend, the reader is referred to the web version of this article.)

lowering of the river base level has induced a strong incision and the present-day Nodda Canyon forms a natural trench – more than 60 m deep and 2 km long – through the Riasi thrust splay (Fig. 6). Downstream, the stratigraphic thickness of the alluvial fan (F1N, Fig. 2) is more than 50 m. The top of the fan has an average slope of 5 ± 1% toward the south, which locally increases to almost 50% at two tectonic scarps above two active faults, the Rain fault and Scorpion fault which are described in section 3.2. The fan also developed above the Tea fault and Spring faults (Fig. 6a) and these two faults do not strongly offset its top.

Upstream, the fan is not continuous: the apex of the fan is preserved but its lower boundary is delineated by the Pillar fault. The slope at the apex is more than 10% and is close to the Pillar fault; the base of the alluvial fan is tilted ~60° to the south. The OSL dating results (Vignon et al., 2016) suggest an age of 14 ± 2 ka BP for the base of the lower part (Fig. 6b) and 15 ± 1 ka BP for the top of the apex. Therefore, the deposits of the fan are all in the range of 13–16 ka BP (Vignon, 2011; Vignon et al., 2014, 2016).

A cut-and-fill terrace ("F2N" on Fig. 2) developed within the Nodda fan. It widens downstream and its termination merges westward with a fill-cut terrace deposited by the paleo-Chenab River. At its southern termination, the cut-and-fill terrace lies 50 m above the Chenab River and 10 m below the surface of the alluvial fan. ^{10}Be dating indicates an age of ~4 ka BP (Vignon et al., 2014, 2016) for the abandonment of this surface.

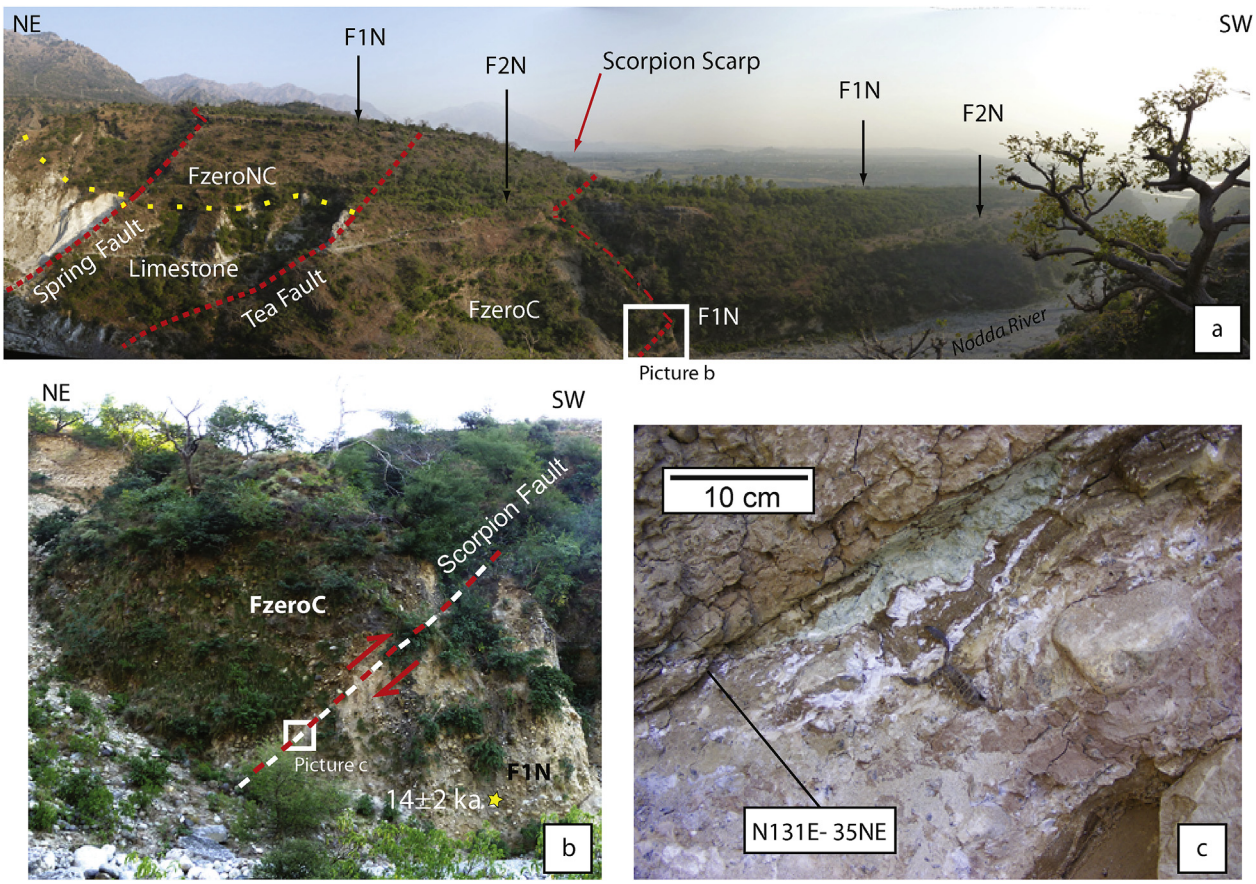

Fig. 6. (a) Picture of the Nodda fan F1N on the left bank of the Nodda River (location in Fig. 4b) The Scorpion scarp, Tea fault and Spring fault are visible; the white box corresponds to the location of Fig. 6b. (b) Picture of the Scorpion fault on the left bank of the Nodda River, thrusting the Chenab deposits Czero over the base of the Nodda fan F1N; the fault plane is N131, 35NE; the white box corresponds to the location of Fig. 6c; yellow star for the OSL sample dated at 14 ± 2 ka. (c) Picture of the fault plane of the Scorpion fault with deformation structures. The scale is given by the Scorpion fault. (For interpretation of the references to colour in this figure legend, the reader is referred to the web version of this article.)

Please cite this article in press as: Mugnier, J.-L., et al., A complex thrust sequence in western Himalaya: The active Medlicott Wadia Thrust, Quaternary International (2017), http://dx.doi.org/10.1016/j.quaint.2017.05.028

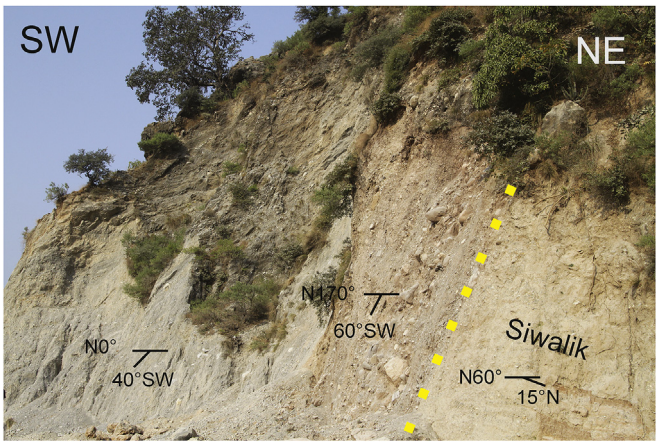

Fig. 7. Tilted deposits at the hangingwall of the Pillar fault (close to the branch line between the Tea and Pillar faults; location in Fig. 2a). These deposits are described as part of the Vaishno Devi Formation (Thakur et al., 2010) in the lower stratigraphic part of the Nodda fan. They are composed of angular pebble-size clasts of limestone in a calcitic consolidated matrix and exhibit the same facies as the Nodda fan deposits. Sedimentary evidence of river transport (layered silty levels with rounded pebbles) is observed locally and indicates a gentle slope during deposition.

3. Geometry of the faults in the Riasi thrust zone

The Riasi thrust fault zone is located at the front of the limestone relief and it is usually difficult to identify in the field due to mass wasting processes. The tectonic contact is located between limestones and Quaternary sediments and dips slightly more gently than the limestone beds that generally strike N090°E with a 65°N dip. The Riasi thrust fault zone is formed in the Riasi cartographic recess by a splay of five faults (Fig. 4): the Pillar and Spring faults affect the limestone sheet, the Tea fault is at the base of the limestone sheet, whereas the Scorpion and Rain faults affect the Cenozoic deposits. To the west, they branch off an oblique ramp; to the east, they branch off the thrust fault, as observed by Thakhur et al. (2010). The name "Riasi thrust" is restricted to the contact at the base of the limestone thrust sheet only.

3.1. Pillar and Spring faults in the Precambrian limestones

The Pillar fault runs nearly parallel to the bedding of the limestone and splits a Chenab unit deposited above the hangingwall spur (HzeroCbis in Fig. 2), with the northern part ~15 m above the southern part. Between the Nodda and Agharnala Rivers, the fault separates the upstream part of the Nodda alluvial fan from its downstream part; the scarp is highly dissected in this area but its height could reach 56 m. To the east of the Nodda fan, Quaternary deposits are tilted more than 30° southwestward in the hangingwall of the Pillar fault (Fig. 7).

The Spring fault is a bedding-parallel fault. It vertically offsets the strath surface at the top of the limestone by 8 m and mildly affects the surface of the Nodda fan on the left bank of the Nodda River (Fig. 6).

The Pillar and Spring faults were probably very active between 14 ka and 36 ka because the units Hzero C and FzeroNC deposited at ~36 ka oin both the hangingwall and footwall of these faults are presently vertically offset by ~200 m.

3.2. Scorpion and Rain faults in the Cenozoic deposits

Two major scarps affect the surface of the lower part of the Nodda fan (Fig. 8). The upstream scarp is linear, trending NW–SE. It

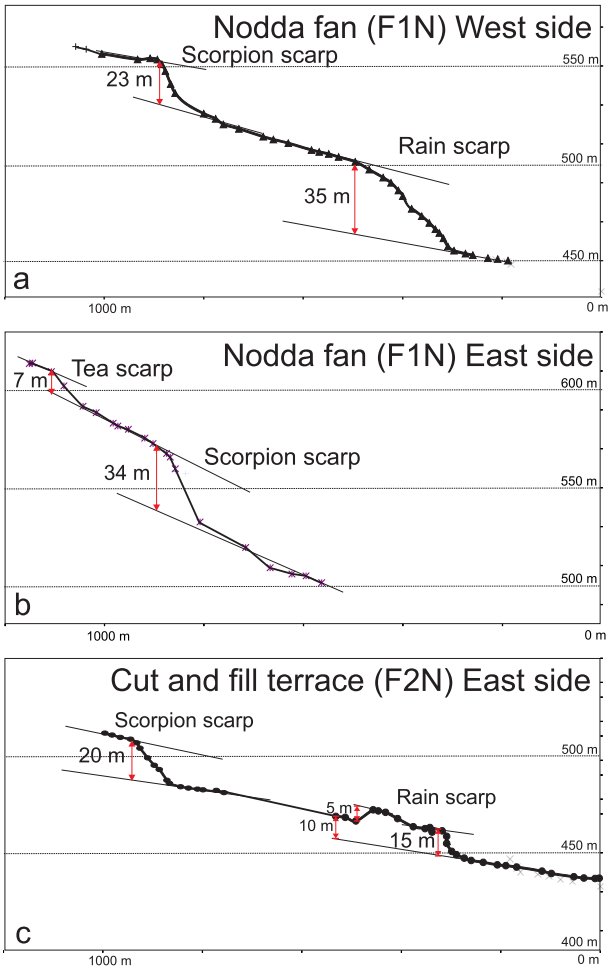

Fig. 8. Topographic profiles through the tectonic scarps. a) The surface of the Nodda fan on the west side of the Nodda River is affected by the Scorpion scarp and Rain scarp. b) The surface of the Nodda fan on the east side of the Nodda River is affected by the Tea scarp and Scorpion scarp. c) The surface of the fill-and-cut unit on the east side of the Nodda River is affected by the Scorpion scarp and Rain scarp.

is 23 m high to the west of the Nodda fan and 34 m to the east of the Nodda River. This scarp also vertically offsets the cut-and-fill surface (F2N in Fig. 8c) by 20 m.

The downstream scarp is spatially curved, matching the isoaltitude lines linked to the downstream spreading of the fan. The scarp is 35 m high on the right side of the Nodda River and the cut-and-fill surface (Fig. 8c) is vertically offset by 15 m on the left side of the river.

The upstream tectonic scarp corresponds to the Scorpion fault. At the base of the canyon, Chenab deposits thrust over the Nodda fan deposits (Fig. 6a) along a fault plane orientated N131°E–35°E. In the footwall, the sediment deposited by the paleo-Nodda River is slightly deformed into a meter-scale normal drag fold. The fault is formed by highly sheared lenses, a few decimeters thick (Fig. 6c) where a mean N163°E–60°E cleavage (Fig. 9) is observed. The motion of the hangingwall (Vialon et al., 1976) is therefore N257°E with a sinistral oblique slip component.

The downstream tectonic scarp is the emergence of the Rain fault. The fault dips 22 ± 3°N at the base of the canyon; sediments at the hangingwall are folded close to the surface in a ramp-flat anticline (e.g. Boyer and Elliot, 1982) while footwall sediments dip gently southward (Fig. 10). The pole perpendicular to the fold axis is estimated at N 29°E (Fig. 9) from measurements of the folded

Please cite this article in press as: Mugnier, J.-L., et al., A complex thrust sequence in western Himalaya: The active Medlicott Wadia Thrust, Quaternary International (2017), http://dx.doi.org/10.1016/j.quaint.2017.05.028

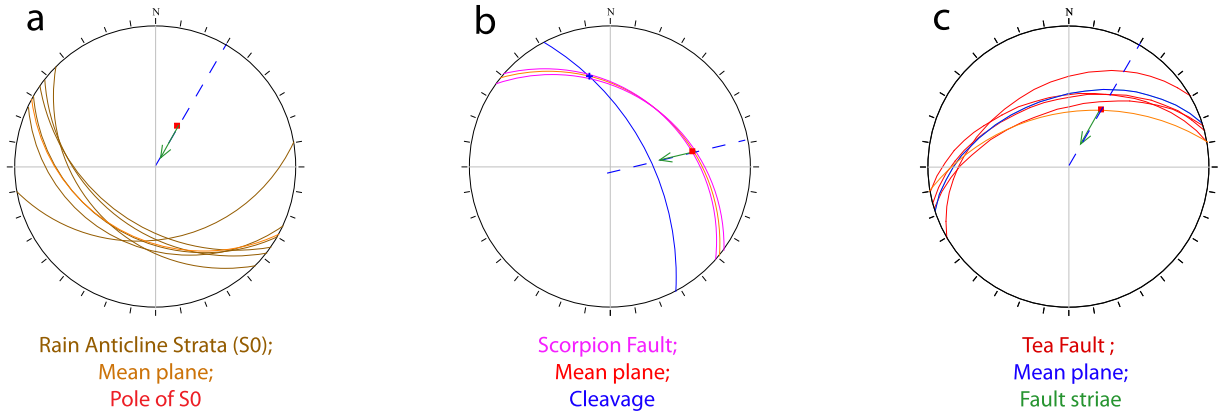

Fig. 9. Microstructural analysis of the fault zones. Fault/striations/cleavage/strata planes for the Wulf stereographic projection on the lower hemisphere. The colors of the lines refer to the colors of the caption. The motion of the hangingwall of the thrust is shown by the dashed blue line. a), b) and c) refer to the southern flank of the Rain anticline (Fig. 10), Scorpion fault (Fig. 6) and Tea fault on the right bank of the Nodda River (Fig. 5), respectively. (For interpretation of the references to colour in this figure legend, the reader is referred to the web version of this article.)

beds and suggests a N29°E- N209°E shortening.

The N257°E motion of the hangingwall observed along the Scorpion fault is slightly different from the one deduced from the N210°E striations observed on the Tea fault. As the latter is coherent with the shortening direction inferred from the trend of the Rain fault anticline and with the regional shortening direction inferred from earthquake mechanisms and GPS measurements (Jouanne et al., 2014), a general N210°E thrust motion is assumed in Section 4.

3.3. Tea fault at the base of the limestone sheet

The Tea fault is observed on the right (Fig. 5) and left (Fig. 6) banks of the Nodda River where it strikes N72°E and N130°E and dips 48°N and 30°N, respectively. Striations were observed on pebbles in the fault zone and their projection is N30°E on the horizontal plane (Fig. 9), coherent with a thrust motion toward N 210°E.

On the left side of the river the limestones thrust at least by

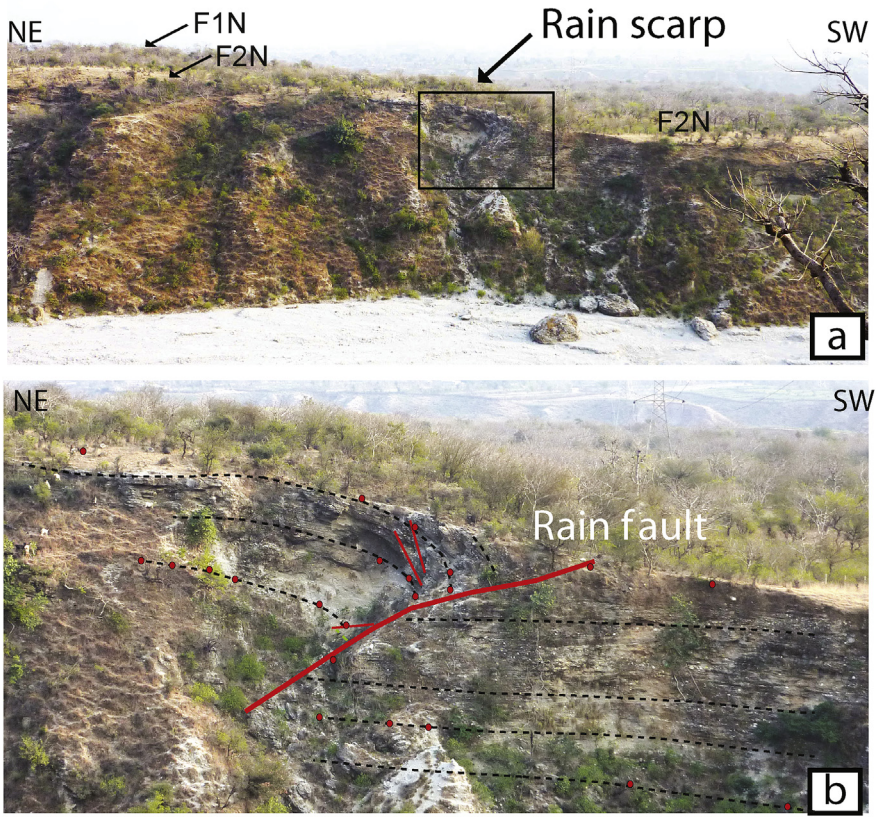

Fig. 10. (a) Picture of the Rain fault and associated tectonic scarp on the left bank of the Nodda River. Location on Fig. 4b). The black box in (a) corresponds to Fig. 8b; the red dots in (b) refer to the total station measurements used for the cross-section in Fig. 12; the black dashed lines correspond to the sedimentary layers. (For interpretation of the references to colour in this figure legend, the reader is referred to the web version of this article.)

Please cite this article in press as: Mugnier, J.-L., et al., A complex thrust sequence in western Himalaya: The active Medlicott Wadia Thrust, Quaternary International (2017), http://dx.doi.org/10.1016/j.quaint.2017.05.028

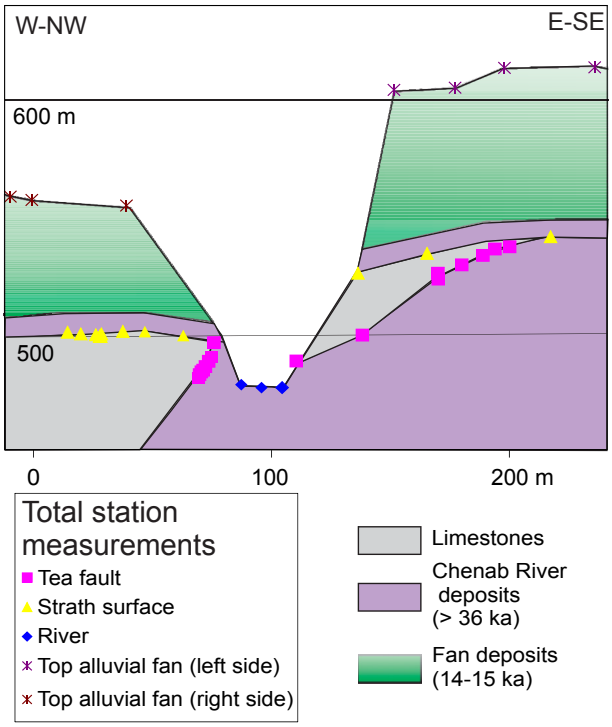

Fig. 11. A cross-section transverse to the Nodda Canyon and close to the Tea fault (strike of the cross-section: N110°E).

124 m (with 62 m vertical throw) onto the lower Chenab units (the FzeroC unit in Fig. 6). The top of the Nodda fan deposits is slightly shifted; the scarp, which is strongly dissected, is ~7 m high.

On the right bank of the Nodda River, the Tea fault shifts (~4 m) the base of the upper Chenab unit (FzeroNC in Fig. 5) but not the top of the Nodda fan. At the footwall of the Tea fault, the Chenab beds dip ~20° northward, whereas the strath surface in its hangingwall dips only a few degrees. We therefore suggest that the Tea fault and the lower Chenab unit were locally tilted ~15° northward prior to deposition of the upper Chenab unit.

The comparison between the western and eastern sides of the Nodda Canyon (Fig. 11) indicates a tilt with an axis parallel to the thrust transport direction. This tilt occurred after the Nodda fan was deposited because it induced a relative uplift of ~50 m on the eastern side, both for the top of the fan and for the strath surface at the top of the limestone. This tilt was presumably related to an increase in the displacement toward the east along the Scorpion fault located at the footwall and close to the Tea fault.

4. Discussion

The Riasi thrust splay is located in a recess and is not cylindrical. Therefore lateral variations in the amount of local thrusting induce bed tilting to the east or west (Fig. 11) and the cross-section restoration performed in the following must be considered as an approximation of the thrust kinematics. Nonetheless, a balanced cross-section provides a reasonable estimate of shortening when it is performed parallel to the transport direction and when the lateral projection distances are short (e.g. Dahlstrom, 1969).

4.1. Geometry of the thrust splay

A cross-section (Fig. 12) located to the east of Nodda River is therefore balanced parallel to the inferred N210°E thrust transport direction. The present-day geometry of the faults and limits of the sedimentary units are mainly based on the total station measurements for the left bank of the Nodda River (Fig. 12b). Some data are nonetheless projected from the right bank of the Nodda River. Furthermore, the northern part of the cross-section is shifted eastward in order to cross the upper part of the Nodda fan (H1N).

This balanced cross section is in line with all of the available data and is both constructed and analyzed to ensure that retro-deformation is geometrically possible and geologically admissible (Dahlstrom, 1969); the additional assumptions involved in this balanced cross-section are explained below:

(a) It is assumed that rigid translation occurs along planar faults and Equation (1) links the vertical throw of the hangingwall (V) to the displacement along the fault plane (D), and the dip of the plane (α) (from Jones and Linnser, 1986):

$$V = D \sin\alpha \quad (1)$$

(b) The fault dips more gently than the beds, because the limestone beds dip northward between 45 and 60°, a relationship that is inferred in the cases of a breach-back thrust (Butler, 1982) cutting through previously tilted structures. At medium depth (a few hundred meters), the Riasi thrust is probably as steep as the central branch of the superficial splay (i.e. close to 45°).

(c) At depth, the branch pattern of the faults is inferred from all of the available surface and sub-surface data and the extrapolation of the superficial dips of the four internal faults. The branch pattern proposed in this cross-section is consistent with the cartographic branch points (Diegel, 1986). The Spring, Tea and Scorpion faults form a splay at a superficial level (less than 600 m in depth), the Rain fault branches onto the Scorpion fault and the Pillar fault branches at greater depth.

(d) Folds develop where the dip of a fault changes. The kink fold model (Suppe, 1983) is used for the folds in the limestones, assuming a shear parallel to the bedding structure indicated in Fig. 12a.

(e) For the Rain fault, it is assumed that the fold in its hangingwall is associated with a flattening at depth from a superficial ramp with a 22° dip to a gentler 15° dip segment. The dip of 15° for the deep segment of the Rain fault is estimated from equation (1); 10 m of uplift is measured for the cut-and-fill terrace (F2N) north of the Rain anticline (Fig. 8c); displacement along this segment is estimated from the displacement along the upper fault segment and an attenuation coefficient (displacement along the upper segment divided by the displacement along the lower segment) estimated at 1.05 based on the work of Suppe (1983, his Fig. 12); the displacement along the upper segment with a dip of 22° was estimated (Equation (1)) at 40 m from the 15 m induced uplift.

(f) A flattening of the faults very close to the surface is highlighted in Fig. 10 and in trenches throughout the Scorpion and Rain fault scarps (Vassallo et al., 2013). This flattening controls the scarp development and specific balancing procedures for the scarps are proposed (Jayangondaperumal et al., 2013). Nonetheless, the vertical simple shear model alone has been used (Jones and Linnser, 1986), as this simplification does not affect the balancing at the scale of the thrust splay and can be used to estimate the vertical throw from the height of the scarp corrected from the general dip of the surface (Fig. 8 and Hanks and Andrews, 1989).

Please cite this article in press as: Mugnier, J.-L., et al., A complex thrust sequence in western Himalaya: The active Medlicott Wadia Thrust, Quaternary International (2017), http://dx.doi.org/10.1016/j.quaint.2017.05.028

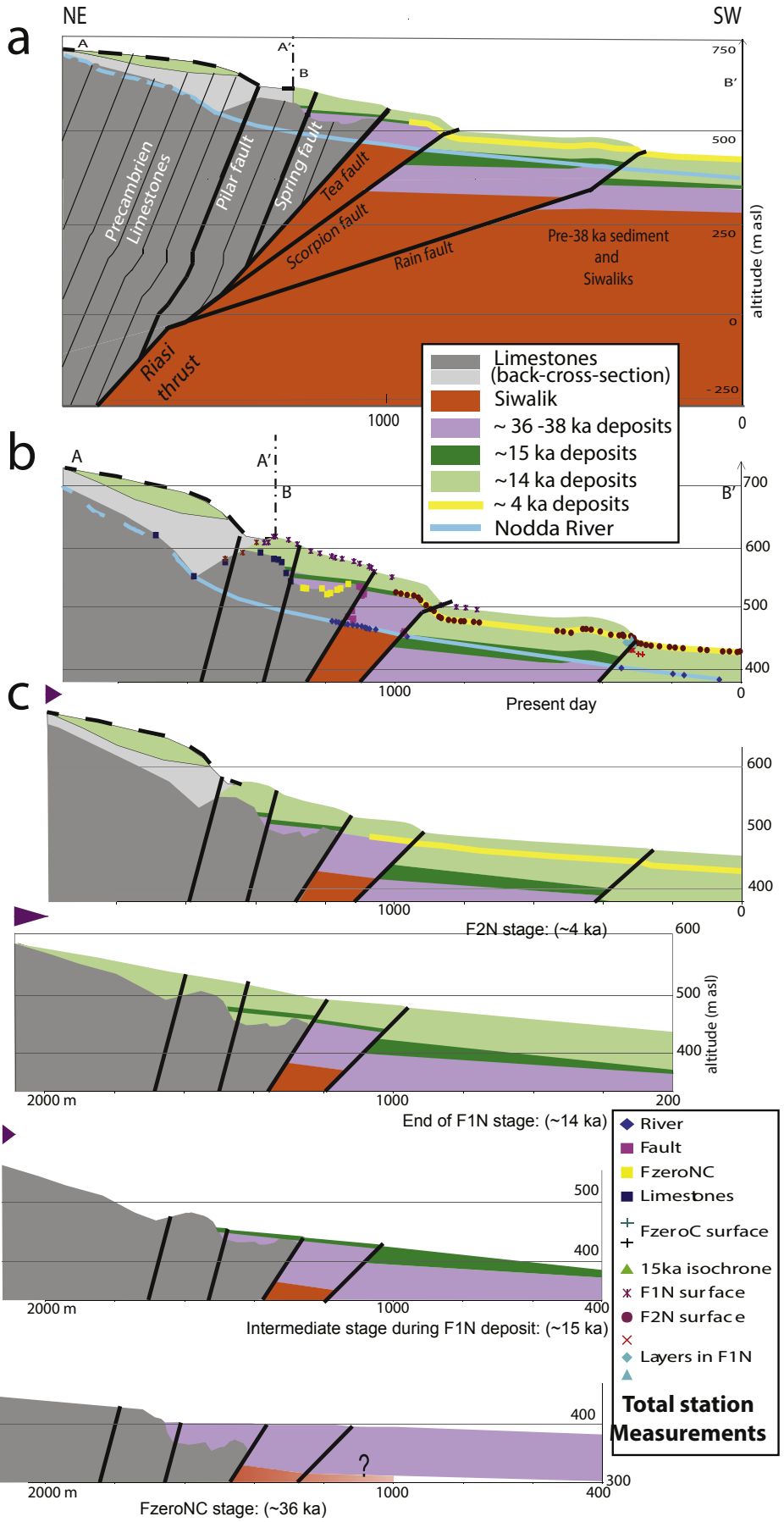

Please cite this article in press as: Mugnier, J.-L., et al., A complex thrust sequence in western Himalaya: The active Medlicott Wadia Thrust, Quaternary International (2017), http://dx.doi.org/10.1016/j.quaint.2017.05.028

4.2. Total deformation of the Nodda fan by the Riasi thrust splay

The present-day vertical separation between the apex and the lower edge of the fan (separated by a horizontal distance of 2 km) is 300 m and is the sum of the vertical tectonic throw and the initial separation due to the slope of the fan. Assuming that the mean slope of the fan was smaller than the present-day slope of the Nodda River (9%) but that the steepening of the river, linked to its increase in energy since the fan deposit, only partly explains the downstream incision of the Nodda fan (~60 m) by the present-day Nodda River, this mean slope ranged between 6 and 9%. The initial vertical separation between the apex and lower edge of the fan was between 120 and 180 m and the total vertical throw since the deposition of the Nodda fan (~14 ka BP) is between 180 and 120 m. The uplift rate is then 9.3 ± 2 mm/yr, close to the 10.6 (±2) mm/yr mean uplift rate found by Vignon et al. (2016) for the present-day to the ~36 ka period based on the differences in incision (Carcaillet et al., 2009) between the footwall and hanging wall terraces of the Chenab River (FzeroC and HzeroC units, respectively, in Fig. 4b). In order to take the results of these two distinct methods into account, a mean uplift rate of 10 mm/yr and a total vertical throw of 140 m are therefore retained in the following for the progressive retro-deformation of the thrust splay (Table 2 and Fig. 12).

For a known V value, a minimum displacement rate is obtained from equation (1) if the estimate of the dip is maximized. For the portion of the Riasi thrust located beneath the branching points, the cumulative displacement rate for the entire fault system is deduced from Equation (1) and is applied to the uplift at the trailing edge of the cross-section; the maximum inferred dip and vertical throw rate are 45° and 9.3 ± 2 mm/yr respectively and the minimum displacement rate is therefore 13.1 (±2.8) mm/yr. This value is close to the 15 (±2.8) mm/yr mean rate independently found by Vignon et al. (2016) for the present-day to ~36 ka period.

4.3. Progressive deformation of the Nodda fan

We performed a progressive restoration based on a kinematic model (e.g. Endignoux and Mugnier, 1990) (Fig. 12c). This restoration is based on the succession of stages marked by sedimentary units: 1) the cut-and-fill surface within the Nodda fan (~4 ka BP), 2) the top of the Nodda fan (~14 ka BP), 3) the lowest level of the fan that presently crops out at the footwall of the Scorpion fault (~15 ka BP), and 4) the top of the Chenab unit (FzeroNC at ~36 ka BP). The uncertainties of the ages are in the order of 1 ka, based on the estimations of Vignon et al. (2014, 2016) and Vassallo et al. (2015).

Most of the geometric data are provided by a detailed topographic study performed with a total station topographic leveling on the eastern side of the Nodda Canyon (Fig. 12 b). For the first time period (0–4 ka), the vertical throw is estimated from the high of the scarps of each fault; for the 4–14 ka time period, it is estimated from the difference between the vertical throws of the 4 ka and 14 ka surfaces. For the other periods (14–15 ka and 15–36 ka), other data come from the changes in the stratigraphic thickness of the units and from the vertical throw of the uppermost unit (HzeroC).

Numerous data have been projected on a single cross-section to estimate the incremental vertical throws and the lack of cylindricity of the structures makes this 2-D restoration not very accurate. We consider that the total throw of the cross-section is less affected by the lateral evolution of the structures and its uncertainty (i.e. 30%) is less than the uncertainty regarding the throw along each fault. No numeric estimation of the uncertainties is nonetheless proposed and Table 2 only summarizes the incremental fault throws for a 140 m total vertical throw.

We believe that the large uncertainties regarding the displacement values do not affect the bulk of the sequence chronology in the thrust splay. An in-sequence propagation is found for the Tea, Scorpion and Rain faults while an out-of-sequence reactivation affects the Pillar fault (Table 2). Therefore, several branches are simultaneously activated for intervals of a few thousand years, whereas others are episodically inactive. This type of complex thrusting sequence is also observed in the Siwalik of western Nepal (Mugnier et al., 1998).

4.4. The continuation at depth of the Riasi thrust

The portion of the Riasi thrust beneath the branching points of the splay, at a shallow depth in the order of 0.5–2 km, would dip close to 45°. This dip is steep for a pure thrust, and a decrease in the dip is therefore inferred for deeper segments of the Riasi thrust (Fig. 13). A several kilometer-scale ramp syncline would develop above such a listric thrust geometry thrust and induce a decrease of the uplift towards the north. The changes in the basal thrust dip induces a hanging-wall deformation and variations in the displacement along a thrust at deeper levels (Huyghe and Mugnier, 1992; Mugnier et al., 2006). The two end-members models for the attenuation at a change of dip of the basal thrust are the shearing parallel to the fault model (Suppe, 1983) and the vertical shearing model (Jones and Linnser, 1986); the ratio between the slip on the basal detachment versus the slip on a ramp is one for shearing-parallel-to-the-fault model (Suppe, 1983) or cosinus ɵ (where ɵ is the change in dip between the basal detachment and the steepest part of the ramp) for the vertical shearing model (Jones and Linnser, 1986). Taking into account a 45° change in dip between the basal detachment and the steepest ramp and a displacement rate of 13.1 (±2.8) mm/yr along the ramp, the displacement rate along the flat MHT is between 7.3 and 15.9 mm/yr (Table 3). The displacement transferred from the flat MHT to the Riasi thrust (Fig. 13) is therefore difficult to quantify precisely and we only conclude that the Himalayan convergence absorbed by the MWT is in the order of 10 mm/yr.

The depth of the branching point between MWT and MHT is still conjectural. In the Central Himalaya (Hirschmiller et al., 2014) and until the longitude of 76°E (Rajendra Prasad et al., 2011), the MHT is usually located at the boundary between the basement and cover. Nonetheless, as the Precambrian limestones at the hangingwall of the Riasi thrust were part of the foreland basement (Srinivasan and Khar, 1996), the basal detachment in the studied area has to be located deeper than the basement/cover interface. Furthermore, this basal detachment is stratigraphically deeper than the Eocambrian salt detachment found westward in the Salt Range area (Jaumé and Lillie, 1988) but not found in Kashmir at the boundary between the Precambrian and younger (here Cenozoic) sediments.

The hypocenter and focal mechanism of the 2005 AD Kashmir earthquake (Avouac et al., 2006) indicate that the MWT still dips ~30° at a depth of 15 km. The post-seismic displacement following this earthquake (Jouanne et al., 2011, 2014) is interpreted as creep along a gently dipping portion of the MHT located at a depth

Fig. 12. Structural and stratigraphic evolution of the Riasi thrust splay (location of the cross-section in Fig. 2a). (a) Branched pattern of the present-day fault at depth (same horizontal and vertical scale). (b) Present-day cross-section drawn from the measured points with the total station on the left bank of Nodda River. The vertical scale magnified by 2. AA' (thick dashed surface line and light grey limestone on the present-day stage) is horizontally offset by 0.5 km from cross-section BB'. The topography of AA′ is extracted from ASTER DEM and the topography of BB′ is measured with the total station. (c) Progressive restoration of the tectonic activity of the Riasi thrust splay. Length of the arrows on the left side between the different stages refer to the incremental horizontal shortening.

Please cite this article in press as: Mugnier, J.-L., et al., A complex thrust sequence in western Himalaya: The active Medlicott Wadia Thrust, Quaternary International (2017), http://dx.doi.org/10.1016/j.quaint.2017.05.028

Table 2
Vertical throw inferred along the different faults and used for the progressive kinematic retro-deformation of Fig. 14b. Most of the geometric data are provided by a detailed topographic study of the eastern side of the Nodda Canyon (bold characters associated with these values). Other data also come from: [w] a projection from the west side; [ff] value estimated from the offset between HzeroC and FzeroC from Vignon et al. (2016); [£] no direct data but the activity has been inferred to maintain the total uplift rate at a value of 10 mm/yr; [*] the development of the Rain fault is assumed in sequence and related to the deposit of the Nodda fan; [$] the activity of the spring and Pillar fault are arbitrarily assumed to be equal.

Time interval	Vertical throw (m)						
	Actual to ~4 ka	Actual to ~14 ka	Actual to ~36 ka	~4 ka to ~14 ka	~14 ka to ~15 ka	~15 ka to 36 ka	~36 ka to ~38 ka
Rain fault	**15**	**35**	35	20 [w]	0[£]	0[*]	0[*]
Scorpion fault	**20**	**34**	51	**14**	**6**	**11**	0 [£]
Tea fault	0[£]	**7**	44	**7**	**4** [w]	**33**	**18**[w]
Spring fault	0[£]	**8**	101	**8**	0	93 [$]	2 [£]
Pillar fault	5 [£]	**56**	149	51[£]	0[£]	93 [$]	0 [£]
Total of the splay (m)	40	**140**	**380**[ff]	100	**10**	230	20

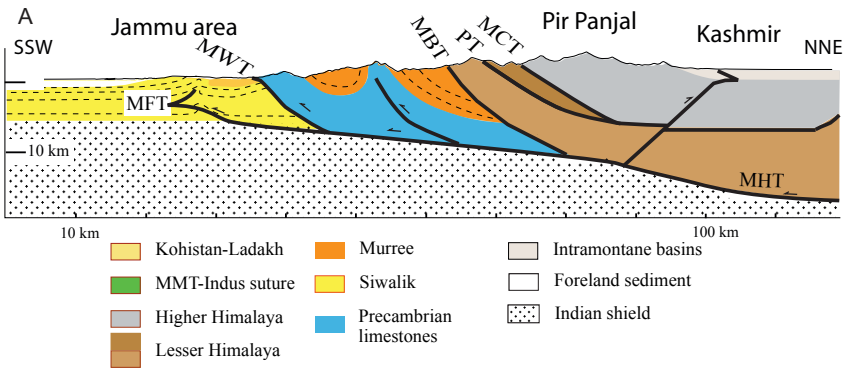

Fig. 13. An interpretative crustal scale cross-section in the Jammu-Kashmir area.

between 15 km and 30 km beneath the Kashmir Basin. In the Central Himalaya, the 2015 Gorkha earthquake occurred on a gently dipping segment located at a depth of only ~10 km (Sreejith et al., 2016). Therefore the MHT is located at a deeper level in the Kashmir-Jammu area than in the Central Himalaya.

4.5. The active tectonics of the western Himalaya

The segment of Himalaya between the 2005 and 1905 earthquakes has been affected for the past several millions year by a convergence rate of 10–14 mm/yr; this value is estimated from the shortening provided by balanced cross-sections (Srinivasan and Khar, 1996) and their time evolution is estimated from the tectonic/sedimentation relationships (Powers et al., 1998) or thermal cooling induced by the tectonics (Meigs et al., 1995). The convergence rate is also estimated from the evolution of the foreland basin in a flexural model coupled with the kinematics of the thrust belt (Mugnier and Huyghe, 2006). Furthermore, the present-day deformation field suggests a convergence rate equivalent to 14–16 mm/year (Jade et al., 2004; Schiffman et al., 2013; Jouanne et al., 2014). During the late Quaternary, in the Riasi area, the Main Boundary Thrust ceased moving at least ~30 ka ago whereas the total shortening rate absorbed by the Medlicott–Wadia Thrust and Main Frontal Thrust over the last 14–24 ka is 11.2 ± 4 and 9.0 ± 3 mm/yr, respectively (Vassallo et al., 2015).

Table 3
Vertical throw and horizontal shortening inferred for the whole splay (assuming a trailing ramp that dips 45°). The minimum displacement rate along the MHT is inferred from a vertical simple shear model (Jones and Linnser, 1986) at the flat/ramp transition. The maximum displacement rate along the MHT is inferred from the preservation of the displacement at the flat/ramp transition. [ff] The present-day to ~36 ka mean rates are estimated by Vignon et al. (2016) from the uplift of the highest terrace of the Chenab (HzeroC unit on Fig. 2b).

Time interval	0 ka to ~14 ka	0 ka to ~36 ka
Vertical throw of the splay (m)	140 (−20/+40)	380[ff]
Vertical throw rate (mm/yr)	9.3 (±2)	10.6 (±2)
Displacement rate (mm/yr)	13.1 (±2.8)	15 (±2.8)
Horiz. short. rate for the splay (mm/yr)	9.3 (±2)	10.6 (±2)
Min. displacement rate along the MHT	9.3 (±2)	10.6 (±2)
Max. displacement rate along the MHT	13.1 (±2.8)	15 (±2.8)

The displacement along the MWT is possibly slightly enhanced in the Chenab recess, which bends the Himalayan structures, by an extra oblique component (Vassallo et al., 2015). Nonetheless, this recess mainly affects the propagation of the frontal Himalayan deformation, leading to the sharp bend in the frontal structure, whereas the MWT is less bent. If a pre-existing basement structure causes this recess (Marshak, 2004), it would also have affected the initial geometry of the MWT and at least partly caused its bending. Therefore, even if a pre-existing structure could work as an asperity along the basal detachment (Mugnier et al., in press) that would locally reduce the activity of the frontal structure and transfer a part of the frontal activity to the MWT, this one is a major thrust outside the recess.

Further east, in the Kangra area, half of the convergence is also out-of-sequence (Thakur et al., 2014) and the local expression of the MWT is represented by the Palampur and Bilaspur thrusts.

Westward, the 2005 earthquake occurred along the Balakot Bagh fault segment of the MWT and extended beneath the western syntax as a thrust wedge (Bendick et al., 2007). The Balakot Bagh fault only releases a small part of the convergence (2–4 mm/yr from Kondo et al., 2008) whereas, based on a geomorphologic study performed close to Mangla (location in Fig. 1b), the MFT accommodates a significant slip rate of at least 10 mm/yr in the core of the western syntax (Cortés-Aranda et al., in press). The Balakot Bagh fault is located further west than the abrupt bend of the Himalayan

Please cite this article in press as: Mugnier, J.-L., et al., A complex thrust sequence in western Himalaya: The active Medlicott Wadia Thrust, Quaternary International (2017), http://dx.doi.org/10.1016/j.quaint.2017.05.028

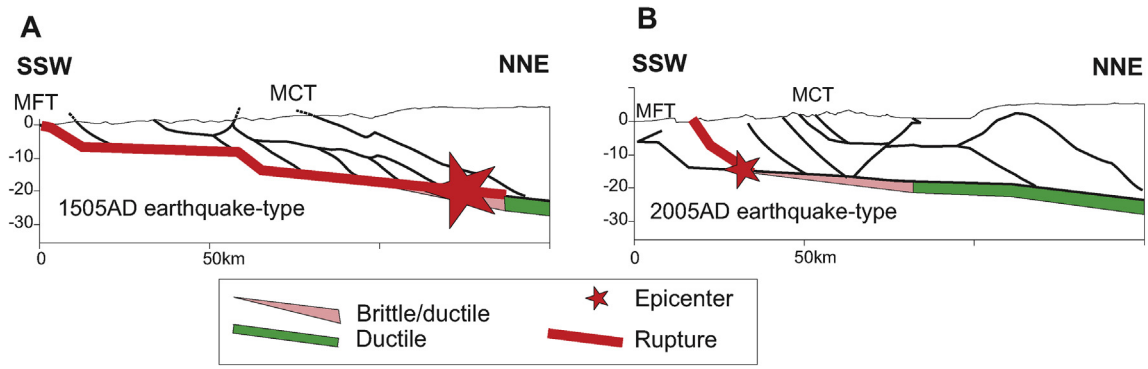

Fig. 14. Implications at the crustal scale of the geometry of the thrusts on the seismic ruptures (adapted from Mugnier et al., 2013) (a) In thin-skinned thrust belts (Central Himalaya, western Nepal), flat detachments are located in the brittle part of the crust resulting in large ruptures and earthquakes greater than Mw 8. This is illustrated by the 1505AD earthquake. (b) In thick-skinned thrust belts (Western Himalaya), ramp cuts through the whole brittle crust and branches off the ductile (or brittle/ductile detachment) result in small ruptures and earthquakes less than Mw 8.

frontal structure that formed by the transition between the Salt Range Thrust and the MFT. Therefore, the deformation could be transferred from the MWT to the frontal structure on the eastern side of the western syntax between Kotli, Mangla and Balakot (Fig. 1b). Therefore, the MWT has a smaller slip rate in the westernmost region.

4.6. Seismic hazard implications

Several studies have suggested that the tectonic structure of the Himalaya is different in its eastern and western portions (Berger et al., 2003; Robert et al., 2011; Mugnier et al., 2011; Mukherjee et al., 2012; Jouanne et al., 2016). The Eastern Himalaya has experienced great historical earthquakes, with magnitudes reaching Mw 8.4 (e.g. Mugnier et al., 2013), but the historical earthquakes in the western Himalaya have never exceeded Mw 7.8: the latest historical earthquakes in the western Himalaya were the 2005 and 1905 events with magnitudes of Mw 7.6 (Kaneda et al., 2008) and 7.8 (Molnar, 1987), respectively. Is this lateral discrepancy fortuitous or does it reflect a lateral variation in the seismo-tectonic characteristics of the Himalaya? This question is important for assessing the seismic hazard in the surrounding areas where large cities like Jammu (India) or Gujranwala (Pakistan) and hydroelectric dams (such as the Mangla Dam) on the Himalayan Rivers are located.

Using geometric data on the continuation of the thrusts to deep in the crust, Coward (1983) suggested separating thrust tectonics into thick-skinned and thin-skinned classes. This distinction has important rheological implications: depending on the depth of the detachment, either the ramps branch off ductile detachments or the flat parts of the thrust planes are in the brittle regime. It also has major seismic implications, with either small or large locked segments of active thrusts, which provide small or large seismic ruptures that directly control the magnitude of the earthquakes. The Central Himalaya is a rather thin-skinned thrust belt where a large portion of the flat is in the brittle regime (Jouanne et al., 2004) and is affected by great earthquakes; this is illustrated by the 1505 AD earthquake (Fig. 14a, adapted from Mugnier et al., 2013) that ruptured the front (Yule et al., 2006) and had an epicenter north of the High Himalaya (Ambraseys and Jackson, 2003) or by the gently dipping rupture of the Gorkha 2015 earthquake (Avouac et al., 2015). The Kashmir 2005 earthquake rupture occurred on the high-angle portion of the Balakot-Bagh fault (Avouac et al., 2006), and did not affect the flat detachment at depth that crept during the post-seismic period (Fig. 14b, adapted from Jouanne et al., 2011). We suggest that the ~300 km long segment of the Himalaya affected by the MWT is a thick-skinned thrust belt and the MHT is rather ductile north of the MWT branching point. Therefore, the size of earthquake would not be a Mw 8 class, even if the rupture on the detachment goes up to the MFT. Nonetheless, the question remains open, because ruptures could occur north of the MWT branching point (Fig. 14b) along the large transition zone between the brittle and ductile regime, as expected for flat detachments (Mugnier et al., 2013).

In the ~200 km long seismic gap between the 2005 and 1905 events, the last large historical earthquake occurred in 1555 and its magnitude was estimated at ~7.6 (Ambraseys and Douglas, 2004). The 1555 earthquake severely damaged the eastern Kashmir Basin area (Thakur and Jayangondaperumal, 2015) and its rupture zone could extend southeast toward Chamba (Fig. 1b, from Joshi and Thakur, 2016). The 1555 surface rupture is probably located on the MWT (Vassallo et al., 2013). Considering a continuous convergence rate of ~14 mm/yr from the long-term to the present-day periods and the absence of aseismic deformation during the interseismic periods in this external part of the Himalaya (Schiffman et al., 2013; Jouanne et al., 2014), the slip deficit in this segment of the Himalaya would be at least 7 m since 1555. This deficit is greater than the slip deficit inferred in the Kangra zone, Central Nepal or Eastern Himalaya where great earthquakes released elastic energy during the XIXth and XXth centuries. It is in the same order of the slip deficit in western Nepal where the last earthquake occurred in 1505 (e.g. Mugnier et al., 2013). An earthquake of Mw 7.7 is estimated from the slip deficit (Kanamori, 1983), if a rupture is assumed along the 50 km long limestone sheet. An earthquake is expected along the MWT in the Riasi area with a magnitude at least as large as the 2005 Kashmir earthquake, which killed more than 70,000 people.

5. Conclusion

Out-of-sequence deformations are inherent in thrust tectonics and are important to understand the seismicity of collisional orogens such as the Himalaya. The neotectonic study of the Medlicott-Wadia Thrust (MWT) shows that it is an out-of-sequence thrust and has enabled us to quantify its deformation. At a smaller scale, the MWT is locally formed by a splay of five faults affected by a complex thrust sequence. An in-sequence propagation is found for the three southern faults and an out-of-sequence reactivation is found for the northern fault. Furthermore, several branches are simultaneously activated for intervals of a few thousand years, whereas others are activated only episodically. Beneath the deepest branching point, the thrust fault is very steep and the displacement rate is locally

Please cite this article in press as: Mugnier, J.-L., et al., A complex thrust sequence in western Himalaya: The active Medlicott Wadia Thrust, Quaternary International (2017), http://dx.doi.org/10.1016/j.quaint.2017.05.028

13.1 (±2.8) mm/yr. Therefore, more than 7.3 mm/yr of displacement along the flat MHT is transferred to this out-of-sequence thrust and a large part of the 14–16 mm/year convergence in the western Himalaya is not accommodated by the frontal anticline.

This suggests that the out-of-sequence character of the 2005 earthquake in Kashmir was not specific to its location in the core of the Hazara-Kashmir syntax at the western termination of the Himalaya but instead was typical of certain great earthquakes that affect the Himalaya to the west of longitude 77°E. The simple seismo-tectonic model frequently inferred for the Central Himalaya where the surface trace of the great earthquakes is located at the front cannot be applied to the western Himalaya; a more complex seismo-tectonic model that takes out-of-sequence ruptures into account needs to be applied to this region.

Therefore, more investigations are needed to better estimate the seismic hazard in this area. The paleoseismology, active tectonics and geometry of the Himalayan thrust will have to be taken into account to understand the thick-skinned character of the far western Himalayan thrust belt and the origin of the Jammu-Kashmir seismic gap.

Acknowledgments

This research was funded by the ANR Catel (PAKSIS), INSU, and Labex@OSUG 2020 programs (Govt of France). RJ kindly acknowledges financial support from the MoES Project (vide # MoES/P.O.(Seismo)/1/(175)/2013, dated 19/6/14. Govt. of India). RJ and PS also acknowledge partial support from the WIHG Project under the MOU between WIHG and the U. of Savoy Mont Blanc. RJ and PS sincerely thank the Director of the WIHG. R. Thiede, G. Mascle, and C. Sutcliffe reviewed the manuscript carefully.

References

Ambraseys, N., Jackson, D., 2003. A note on early earthquakes in northern India and southern Tibet. Science 84, 571–582.
Ambraseys, N.N., Douglas, J., 2004. Magnitude calibration of north Indian earthquakes. Geophys. J. Int. 159 (1), 165–206.
Avouac, J.P., 2003. Mountain building, erosion, and the seismic cycle in the Nepal Himalaya. In: Advances in Geophysics. Elsevier, pp. 1–80.
Avouac, J.-P., Ayoub, F., Leprince, S., Konca, O., Helmberger, D.V., 2006. The 2005, Mw 7.6 Kashmir earthquake: sub-pixel correlation of ASTER images and seismic waveforms analysis. Earth Planet. Sci. Lett. 249 (3–4), 514–528.
Avouac, J.P., Meng, L., Wei, S., Wang, W., Ampuero, J.P., 2015. Lower edge of locked Main Himalayan Thrust unzipped by the 2015 Gorkha earthquake. Nat. Geosci. ISSN 1752–0894.
Bendick, R., Bilham, R., Khan, A., Khan, F., 2007. Slip on an active wedge thrust from geodetic observations of the 8 October 2005 Kashmir earthquake. Geology 35, 267–270. http://dx.doi.org/10.1130/G23158.
Berger, A., Jouanne, F., Hassani, R., Mugnier, J.L., 2003. Modelling the spatial distribution of present-day deformation in Nepal. How cyclindrical is the Main Himalayan Thrust in Nepal? Geoph. J. Int. 156 (1), 94–112.
Boyer, S.E., Elliot, D., 1982. Thrust systems. Am. Assoc. Pet. Geol. Bull. 66, 1196–1230.
Butler, R., 1982. The terminology of structures in thrust belts. J. Struct. Geol. 4, 239–245.
Carcaillet, J., Mugnier, J.L., Koci, R., Jouanne, F., 2009. Uplift and active tectonics of southern Albania inferred from the incision of alluvial terraces. Quat. Res. 71, 465–476.
Champel, B., Van Der Beek, P., Mugnier, J.L., Leturmy, P., 2002. Growth and lateral propagation of fault-related folds in the Siwaliks of western Nepal: rates, mechanisms and geomorphic signature. J. Geoph. Res. 107 http://dx.doi.org/10.1029/2001JB000578.
Chandra, U., 1992. Seismotectonics of Himalaya. Curr. Sci. 62, 40–72.
Cortés-Aranda, J., Mugnier, J.-L., Vassallo, R., Jouanne, F., Carcaillet, J., Adnan, A., 2017. Holocene shortening rates and seismic hazard assessment for the frontal Potwar Plateau, NW Himalaya of Pakistan: insights from 10Be concentrations on fluvial terraces in the Mahesian Anticline. Quat. Int. http://dx.doi.org/10.1016/j.quaint.2017.02.032 (this special volume) (in press).
Coward, M.P., 1983. Thrust tectonics, thin skinned or thick skinned, and the continuation of thrusts to deep in the crust. J. Strutural Geol. 5, 113–123.
Coward, M.P., Rex, D.C., Khan, A.M., Windley, B.F., Broughton, R.D., Luff, I.W., Petterson, M.G., Pudsey, C., 1986. Collision tectonics in the NW Himalayas. Geol. Soc. Lond. Spec. Publ. 19 (1), 203–219.
Dahlstrom, C.D., 1969. Balanced cross-sections. Can. J. Earth Sci. 6, 743–757.
Diegel, F.A., 1986. Topological constraints on imbricate thrust networks, examples from the Mountain City window, Tennessee, U.S.A. J. Struct. Geol. 8, 269–279.
Feldl, N., Bilham, R., 2006. Great Himalayan earthquakes and the Tibetan plateau. Nature 444 (7116), 165–170.
Gansser, A., 1964. Geology of the Himalayas. Inter Science Publishers, John Wiley & Sons, p. 289.
Hanks, T.C., Andrews, J., 1989. Effect of far-field slope on morphologic dating of scarplike landforms. J. Geophys. Res. 94, 565–573.
Hirschmiller, J., Grujic, D., Bookhagen, B., Huyghe, P., Mugnier, J.L., Ojha, T., 2014. What controls the growth of the Himalayan wedge? Pliocene to recent shortening of the Siwalik group in the Himalayan foreland belt. Geology 142 (3), 247–250. http://dx.doi.org/10.1130/G35057.1.
Hough, S.E., Bilham, R., 2008. Site response of the Ganges basin inferred from re-evaluated macroseismic observations from the 1897 Shillong, 1905 Kangra, and 1934 Nepal earthquakes. J. Earth Syst. Sci. 117, 773–782. http://dx.doi.org/10.1007/s12040-008-0068-0.
Hussain, A., Yeats, R., MonaLisa, H., 2009. Geological setting of the 8 October 2005 Kashmir earthquake. J. Seismol. 13 (3), 315–325.
Huyghe, P., Mugnier, J.L., 1992. Short-cut geometry during structural inversions; competition between faulting and reactivation. Bull. la Soc. Geol. Fr. 163 (6), 691–700.
Jayangondaperumal, R., Mugnier, J.L., Dubey, A.K., 2013. Earthquake slip estimation from the scarp geometry of Himalayan Frontal Thrust, western Himalaya: implications for seismic hazard assessment. Int. J. Earth Sci. Geol. Rundsch. D-12-00254, 1–19.
Jade, S., Bhatt, B.C., Yang, Z., Bendick, R., Gaur, V.K., Molnar, P., Anand, B., Kumar, D., 2004. GPS measurements from the Ladakh Himalaya, India: preliminary tests of plate-like or continuous deformation in Tibet. Geol. Soc. Am. Bull. 116, 1385–1391. http://dx.doi.org/10.1130/B25357.1.
Jaumé, S.C., Lillie, R., 1988. J. Mechanics of the Salt Range–Potwar Plateau, Pakistan: a fold-and-thrust belt underlain by evaporites. Tectonics 7, 57–71.
Jones, H., Linnser, H., 1986. Computer synthesis of balanced cross-sections by forward modelling. Am. Assoc. Pet. Geol. Bull. 70 (5), 605.
Johnson, G., Johnson, N., Opdyke, N., Tahirkheli, R., 1979. Magnetic reversal stratigraphy and sedimentary tectonic history of the upper Siwalik group eastern salt range and southwestern Kasmir. In: Farah, A., DeJong, K. (Eds.), Geodynamics of Pakistan. Geological Survey of Pakistan, Quetta, pp. 149–165.
Jouanne, F., Mugnier, J.L., Gamond, J.F., Le Fort, P., Pandey, M.R., Bollinger, L., Flouzat, M., Avouac, J.P., 2004. Current shortening across the Himalaya of Nepal. Geoph. J. Int. 157, 1–14.
Jouanne, F., Awan, A., Madji, A., Pêcher, A., Latif, M., Kausar, A., Mugnier, J.L., Khan, I., Khan, N., 2011. Postseismic deformation in Pakistan after the 8 October 2005 earthquake: evidence of afterslip along a flat north of the Balakot-Bagh thrust. J. Geophys. Res. 116 (B7), B07401.
Jouanne, F., Awan, A., Pêcher, A., Kausar, A., Mugnier, J.L., Khan, I., Khan, N.A., Van Melle, J., 2014. Present-day deformation of the northwestern Himalaya. J. Geophys. Res. Solid Earth. 119 (3), 2487–2503.
Jouanne, F., Mugnier, J.L., Sapkota, S., Bascou, P., Pecher, A., 2016. Estimation of coupling along the main Himalaya thrust in central Himalaya. J. Asian Earth Sci. http://dx.doi.org/10.1016/j.jseaes.2016.05.028.
Joshi, M., Thakur, V., 2016. Signatures of 1905 Kangra and 1555 Kashmir earthquakes in medieval period Temples of Chamba Region, northwest Himalaya. Seismol. Res. Lett. 87, 1150–1160.
Kanamori, H., 1983. Magnitude scale and quantification of earthquakes. Tectonophysics 93, 185–199.
Kaneda, H., Nakata, T., et al., 2008. Surface rupture of the 2005 Kashmir, Pakistan, earthquake and its active tectonic implications. Bull. Seismol. Soc. Am. 98 (2), 521–557.
Kondo, H., Nakata, T., Akhtar, S., Wesnousky, S., Sugito, N., Kaneda, H., Tsutsumi, H., Khan, A., Khattak, W., Kausar, A., 2008. Long recurrence interval of faulting beyond the 2005 Kashmir earthquake around the northwestern margin of the Indo-Asian collision zone. Geology 36, 731–734. http://dx.doi.org/10.1130/G25028A.
Krishnaswamy, V.S., Jalote, S.P., Shome, S.K., 1970. Recent crustal movements in north-west Himalaya and the Gangetic foredeep and related patterns of seismicity. Symp. Earthq. Eng. 4th Roorkee, 419–439.
Marshak, S., 2004. Salients, Recesses, Arcs, Oroclines, and Syntaxes; a review of ideas concerning the formation of mapview curves in fold-thrust belts. In: Mc Clay (Ed.), Thrust Tectonics and Hydrocarbon System, A. A. P. G. Mem, vol. 82, pp. 131–156.
Meigs, A.J., Burbank, D.W., Beck, R.A., 1995. Middle-late Miocene (>10 Ma) formation of the main boundary thrust in the western Himalaya. Geology 23, 423–426.
Molnar, P., 1987. The distribution of intensity associated with the 1905 Kangra earthquake and bounds on the extent of the rupture zone. J. Geol. Soc. India 29, 221–229.
Mugnier, J.-L., Mascle, G., Faucher, T., 1992. La structure des Siwaliks de l'Ouest Népal : un prisme d'accrétion intracontinental. Bull. Soc. Géol. Fr. 163, 585–595.
Mugnier, J.L., Delcaillau, B., Huyghe, P., Leturmy, P., 1998. The Break-Back Thrust splay of the Main Dun Thrust: evidence for an intermediate displacement scale between seismic/aseismic fault slip and finite geometry of thrust systems. J. Struct. Geol. 20, 857–864.
Mugnier, J.L., Huyghe, P., Gajurel, A., Becel, D., 2005. Frontal and piggy-back seismic ruptures in the external thrust belt of Western Nepal. J. Asian Earth Sci. 25 (5), 707–717.

Please cite this article in press as: Mugnier, J.-L., et al., A complex thrust sequence in western Himalaya: The active Medlicott Wadia Thrust, Quaternary International (2017), http://dx.doi.org/10.1016/j.quaint.2017.05.028

Mugnier, J.L., Huyghe, P., 2006. The Ganges basin geometry records a pre-15 Ma isostatic rebound of Himalaya. Geology 34 (6), 445–448.

Mugnier, J.L., Becel, D., Granjeon, D., 2006. Active tectonics in the Subandean belt inferred from the morphology of the Rio Pilcomayo. In: Willett, S.D., Hovius, N., Brandon, M.T., Fisher, D. (Eds.), Tectonics, Climate and Landscape Evolution, Geol. Soc. Am. Spec. Publ, vol. 398, pp. 353–369.

Mugnier, J.L., Huyghe, P., Gajurel, A., Upreti, B., Jouanne, F., 2011. Seismites in the Kathmandu basin and seismic hazard in central Himalaya. Tectonophysics. http://dx.doi.org/10.1016/j.tecto.2011.05.012.

Mugnier, J.L., Gajurel, A., Huyghe, P., Jayangondaperumal, R., Jouanne, F., Upreti, B., 2013. Structural interpretation of the great earthquakes of the last millennium in central Himalaya. Earth-Science Rev. 127, 30–47.

Mugnier, J.L., Jouanne, F., Bhattarai, R., Cortes-Aranda, J., Gajurel, A., Leturmy, P., Robert, X., Upreti, B., Vassallo, R., 2017. Segmentation of the Himalayan mega-thrust around the 25 April 2015 Nepal earthquake. J. Asian Earth Sci. http://dx.doi.org/10.1016/j.jseaes.2017.01.015 special volume « the Gorka earthquake ».

Mukherjee, S., Koyi, H.A., Talbot, C., 2012. Implications of channel flow analogue models in extrusion of the Higher Himalayan Shear Zone with special reference to the out-of-sequence thrusting. Int. J. Earth Sci. 101, 253–272.

Mukherjee, S., 2015. A review on out-of-sequence deformation in the Himalaya. In: Mukherjee, S., Carosi, R., van der Beek, P., Mukherjee, B.K., Robinson, D. (Eds.), Tectonics of the Himalaya. Geological Society, London, Special Publications, vol. 412, pp. 67–109. http://dx.doi.org/10.1144/SP412.13.

Pêcher, A., Seeber, L., Guillot, S.,F., Jouanne, F., Kausar, A., Latif, M., Majid, A., Mahéo, G., Mugnier, J.L., Rolland, Y., van der Beek, P., Van Melle, J., 2008. Stress field evolution in the northwest Himalayan syntaxis, northern Pakistan. Tectonics 27 (6), TC6005.

Powers, P.M., Lillie, R.J., Yeats, R.S., 1998. Structure and shortening of the Kangra and Dehra Dun reentrants, sub-Himalaya, India. Geol. Soc. Am. Bull. 110, 1010–1027.

Raiverman, V., Chugh, M., Srivastava, A., Prasad, D., Das, S., 1994. Cenozoic tectonic of frontal fold belt of the Himalaya and indo-gangetic foredeep with pointers towards hydrocarbon prospects. In: Biswas, S.K., et al. (Eds.), Proc. Second Seminar on Petroliferous Basins of India, vol. 3. Indian Petroleum Publishers, Dehra Dun, 248001, India, pp. 25–54.

Rajendra Prasad, B., Klemperer, S.L., Rao, V., Tewari, H.C., Khare, P., 2011. Crustal structure beneath the Sub-Himalayan fold–thrust belt, Kangra recess, northwest India, from seismic reflection profiling: implications for Late Paleoproterozoic orogenesis and modern earthquake hazard. Earth Planet. Sci. Lett. 308, 218–228.

Robert, X., van der Beek, P., Braun, J., Perry, C., Mugnier, J.L., 2011. Control of detachment geometry on lateral variations in exhumation rates in the Himalaya: insights from low − temperature thermochronology and numerical modeling. J. Geophys. Res. 116, B05202. http://dx.doi.org/10.1029/2010JB007893.

Schiffman, C., Singh Bali, B., Szeliga, W., Bilham, R., 2013. Seismic slip deficit in the Kashmir Himalaya from GPS observations. Geophys. Res. Lett. 40, 5642–5645.

Seeber, L., Armbruster, J., 1981. Great detachment earthquakes along the Himalayan arc and long term forecast. In: Sibson, D.W., Richards, P.G. (Eds.), Earthquake Prediction: an International Review, Maurice Ewing Series, vol. 4. Geophysical Union, Amer, pp. 259–277. Washington D.C.

Sreejith, K.M., Sunil, P.S., Agarwal1, R., Saji, A., Ramesh, D.S., Rajawat, A.S., 2016. Coseismic and early postseismic deformation due to the 25 April 2015, Mw 7.8 Gorkha, Nepal earthquake from InSAR and GPS measurements. Geophys. Res. Lett. 43, 3160–3168. http://dx.doi.org/10.1002/2016GL067907.

Srinivasan, S., Khar, B., 1996. Status of hydrocarbon exploration in Northwest Himalaya and foredeep- Contribution to stratigraphy and structure. Geol. Surv. Ind. Spl. Pub. 21, 295–405.

Suppe, J., 1983. Geometry and kinematics of fault-bend folding. Amer. J. Sci. 283, 684–721.

Thakur, V.C., Jayangondaperumal, R., Malik, M., 2010. Redefining Medlicott-Wadia's main boundary fault from Jhelum to Yamuna: an active fault strand of the main boundary thrust in northwest Himalaya. Tectonophysics 489 (1–4), 29–42.

Thakur, V.C., Joshi, M., Sahu, D., Suresh, N., Jayangondaperumal, R., Singh, A., 2014. Partitioning of convergence in Northwest Sub-Himalaya: estimation of late Quaternary uplift and convergence rates across the Kangra reentrant, North India. Int. J. Earth Sci. 103, 1037–1056.

Thakur, V.C., Jayangondaperumal, R., 2015. Seismogenic active fault zone between 2005 Kashmir and 1905 Kangra earthquake meizoseismal regions and earthquake hazard in eastern Kashmir seismic gap. Curr. Sci. 109, (3), 610–617.

Vassallo, R., Mugnier, J.L., Jomard, H., Malik, M., Jouanne, F., Buoncristiani, J.F., Jayangondaperumal, R., 2013. Northwestern Himalayan active front: what paleoseismology tells us about very large thrusts. In: 4th International INQUA Meeting on Paleoseismology, Active Tectonics and Archeoseismology (PATA), 9-14 October 2013, Aachen, Germany.

Vassallo, R., Mugnier, J.-L., Vignon, V., Malik, Manzoor A., Jayangondaperumal, R., Srivastava, P., Jouanne, F., Carcaillet, J., 2015. Quaternary deformation and seismic hazard in Northwestern Himalaya. Earth Planet. Sci. Lett. 411, 241–252.

Vialon, P., Ruhland, M., Grolier, J., 1976. Elements de tectonique analytique. Masson, ISBN 2 225 44 286 X, p. 118.

Vignon, V., 2011. Activité hors séquence des chevauchements dans la syntaxe nord-ouest himalayenne : apports de la modélisation analogique et quantification quaternaire par analyse morphotectonique. PHD thesis. University J. Fourier, p. 278.

Vignon, V., Srivastava, P., Vassallo, R., Mugnier, J.-L., Carcaillet, J., 2014. Dating of the Quaternary Terraces Close to the Chenab River (Western Himalaya). PANGAEA® Data Publisher for Earth & Environmental Science. http://dx.doi.org/10.1594/PANGAEA.836910. http://doi.pangaea.de/10.1594/PANGAEA.836910.

Vignon, V., Mugnier, J.-L., Vassallo, R., Srivastava, P., Malik, M., Jayangondaperumal, R., Jouanne, F., Buoncristiani, J.-F., Carcaillet, J., Replumaz, A., Jaumar, H., 2016. Sedimentation close to the active Medlicott Wadia Thrust (Western Himalaya) : how to decipher tectonics and base level changes (Jammu-Kashmir area, India). Geomorphology. Available online 6 August 2016.

Yeats, R.S., Nakata, T., Farah, A., Fort, M., Mirza, M.A., Pandey, M.R., Stein, R.S., 1992. Supplement to. The Himalayan Frontal Fault System: Annales Tectonicae, vol. 6, pp. 85–98.

Yule, D., Dawson, S., Lave, J., Sapkota, S., Tiwari, D., 2006. Possible evidence for surface rupture of the main frontal thrust during the great 1505 Himalayan earthquake, far-western Nepal. EOS Trans. AGU 52 (Fall Meet. Suppl.), Abstract S33C-05.

Zhao, W.J., Nelson, K., 1993. Deep seismic-reflection evidence for continental underthrusting beneath southern Tibet. Nature 366 (6455), 557–559.

Please cite this article in press as: Mugnier, J.-L., et al., A complex thrust sequence in western Himalaya: The active Medlicott Wadia Thrust, Quaternary International (2017), http://dx.doi.org/10.1016/j.quaint.2017.05.028